

**Mid-latitude daily summer temperatures reshaped by soil moisture under climate  
change**

H. Douville<sup>1\*</sup>, J. Colin<sup>1</sup>, E. Krug<sup>1</sup>, J. Cattiaux<sup>1</sup>, S. Thao<sup>1</sup>

<sup>1</sup>*CNRM-GAME, 42 Avenue G. Coriolis, 31057 Toulouse Cedex 01, France*

**\*Corresponding author:** Correspondence or requests should be addressed to Dr. Hervé Douville, CNRM/GMGEC/VDR, 42 avenue Coriolis, 31057 Toulouse Cedex, France. E-mail: herve.douville@meteo.fr

This article has been accepted for publication and undergone full peer review but has not been through the copyediting, typesetting, pagination and proofreading process which may lead to differences between this version and the Version of Record. Please cite this article as doi: 10.1002/2015GL066222

## Abstract

Projected changes in daily temperatures are highly model-dependent, particularly in the summer mid-latitudes where the spread in the response of heat waves represents a major obstacle for the design of adaptation strategies. Understanding the main reasons for such uncertainties is obviously a research priority. Here we use a set of global atmospheric simulations to assess the contribution of the soil moisture feedback to changes in the full distribution of daily maximum summer temperatures projected in the late 21<sup>st</sup> century. Results show that this feedback (i) accounts for up to one third of the mean increase in daily maximum temperatures, (ii) dominates changes in the shape of the distribution, and (iii) explains about half of the increase in the severity of heat waves over densely populated areas of the northern mid-latitudes. A dedicated intercomparison project is therefore needed to assess and constrain land surface feedbacks in the new-generation Earth System Models.

### Key points:

- The soil moisture feedback amplifies the mid-latitude summer warming over land
- The soil moisture feedback dominates changes in the shape of Tmax distribution
- The soil moisture feedback can explain half of the increase in heat wave severity

## 1. Introduction

According to the fifth Assessment Report of the Intergovernmental Panel On Climate Change (IPCC), a future increase in the frequency, duration and intensity of heat waves is considered as *very likely*. Yet, the magnitude of these regional changes remains highly model-dependent [e.g., *Sillmann et al. 2013, Schoetter et al. 2014*] and do not scale very well on the projected global warming [*Clark et al. 2010*]. This is a major obstacle to the design of efficient mitigation and adaptation policies. Mitigation targets are generally described in terms of global and annual mean temperature increase, which is not the only relevant parameter to consider in order to make an informed decision about the sustainable emissions of CO<sub>2</sub>. Adaptation strategies, decided at local to national levels, require regional information about the full temperature distribution. In many land areas, projections of daily temperatures do not simply result in a shift of the distribution [*Hegerl et al. 2004*]. For example, summer temperature extremes over central and western Europe are projected to increase substantially more than the corresponding seasonal mean temperatures, due to an enhanced variability at interannual to intraseasonal time scales [*Schär et al. 2004, Fischer et al. 2012, Volodin and Yurova.2013, Cattiaux et al. 2015*]. Beyond changes in mean and variance, changes in the distribution skewness can also substantially modulate the response of hot extremes [*Volodin and Yurova.2013*].

Thus, changes in the full distribution of daily minimum and/or maximum temperatures need to be further explored and better understood. Cloud feedbacks represent the main source of model uncertainty on the the projected global warming [*Vial et al. 2013*], but their influence on the shape of the temperature distribution has not been investigated so far. Beyond radiative

processes, latent and sensible heat fluxes also play a key role in the surface energy budget. Their continental response to global warming is strongly influenced by soil moisture [e.g., *Boé and Terray 2008, Diffenbaugh and Ashfaq 2010, Seneviratne et al. 2010, Boberg and Christensen 2012*], whose response to climate change is extremely variable depending on the region, the season and the model (e.g., IPCC AR5, Fig. 12.23). Recently, a multi-model sensitivity experiment was conducted to isolate the soil moisture feedback (hereafter SMF) contribution to the land surface warming projected at the end of the 21<sup>st</sup> century [*Seneviratne et al. 2013*]. The methodology consisted in a pair of atmosphere-only 1950-2100 simulations in which soil moisture boundary conditions were prescribed from either a fixed (present-day) or time-dependent (transient) monthly climatology of a reference climate change simulation. Strong and consistent SMFs were found on surface air temperatures, especially for the 95<sup>th</sup> percentile of the daily maximum surface temperatures (Tmax). However, such an experimental protocol may have undesirable effects when switching off the land-atmosphere coupling and the shape of the temperature distribution was not analysed.

## **2. Model and experiment design**

Here we go further and design an original set of less-constrained experiments to quantify the SMF contribution to changes in the full distribution of summer Tmax. The focus is on the boreal mid-latitude land areas, where major crop productions are particularly vulnerable to hot extremes. We use a global climate model and a flexible nudging technique to control the monthly mean soil moisture climatology while permitting significant departures from the climatology at the model time step.

The model consists of the ARPEGE-Climat v6.0 atmospheric GCM coupled to the ISBA-

TRIP 3-layer land surface hydrology and is very close to the land-atmosphere component of the CNRM-CM5 OAGCM that participated in the CMIP5 intercomparison project [Voldoire *et al.* 2013]. Present-day climate simulations cover the 1979-2008 period and use prescribed observed monthly mean sea surface temperature. Future climate simulations focus on the late 21<sup>st</sup> century (2071-2100) and use prescribed future SST computed as the sum of the 1979-2008 SST and the climatological monthly SST anomalies derived from the CNRM-CM5 OAGCM (using the same present-day and future periods). The RCP8.5 concentration scenario was selected to enhance the climate change signal-to-noise ratio and, thereby, avoid the need of ensemble experiments. Radiative forcings were prescribed in accordance with the selected periods and the scenario. A 1-yr to 10-yr spin-up period was used to allow the model equilibrium with the prescribed SST and radiative boundary conditions.

The nudging technique [Douville *et al.* 2001, Douville 2003] is used to control the monthly mean soil moisture climatology in global atmospheric simulations. It was adapted to the tile-approach of the updated ISBA land surface model (each tile is nudged towards its respective soil moisture climatology). The nudging is applied on the total (liquid+solid) water content so that the ratios of liquid and ice water contents were left unchanged in each soil layer. Only the root-zone and deep soil reservoirs are nudged while the upper soil moisture (which is used to diagnose bare soil evaporation) was left interactive. In doing so, we claim that the model is relaxed towards a reference monthly mean climatology while preserving to some extent a physically-consistent soil-atmosphere coupling.

Five 30-yr global atmospheric simulations were performed. The reference simulations, PR and FR for present-day (1979-2008) and future (2071-2100) climates respectively, are driven by prescribed sea surface temperatures (SST) and radiative forcings. They provide a reference estimate of the climate change projected with free-running soil moisture boundary conditions.

Three additional simulations are analysed: a present-day climate simulation nudged towards

the PR soil moisture climatology (PNP), a future climate simulation also nudged towards the PR soil moisture climatology (FNP), and a future climate simulation nudged towards the FR soil moisture climatology (FNF). This original design allows us to split the projected climate change into four contributions:

$$\text{FR-PR} = (\text{FR-FNF}) + (\text{FNF-FNP}) + (\text{FNP-PNP}) + (\text{PNP-PR}) \quad (1)$$

Our focus is primarily set on the SMF contribution (FNF-FNP) and its comparison with the contribution of climate change without the feedback from the mean soil moisture change (FNP-PNP). However, this breakdown also draws attention to the possible side effects of the nudging technique in both present-day (PNP-PR) and future (FR-FNF) climates. Our objective is to control the monthly mean soil moisture climatology (and thereby isolate the long-term SMF) without damping too much the intraseasonal variability. As illustrated by Fig. S1 and as discussed by Douville [2003], our methodology is in this respect less disruptive than an abrupt soil moisture overriding technique. Note that Eq. (1) is similar to the breakdown proposed by Seneviratne et al. (2006) in their regional analysis of land-atmosphere coupling in future vs present-day climate. Yet, our aim is here to compare (FNF-FNP) with (FNP-PNP) while their focus was on the difference between (FR-FNF) and (PR-PNP).

### 3. Results

Fig. 1 illustrates the breakdown of Equation (1) applied to the projected changes in summer mean soil moisture and Tmax over the Northern Hemisphere. In the mid-latitudes, the CNRM model simulates a significant drying and a strong surface warming over the US and eastern Europe. As expected, the reference soil moisture anomalies project almost entirely onto the

FNF-FNP differences. Despite their weak magnitude, the soil moisture differences can be statistically significant in FNP-PNP due to the systematic differences in the land-atmosphere water fluxes (especially precipitation) between present-day and future climates. The reference projected surface warming is mostly explained by the prescribed radiative forcings and SST anomalies (i.e., FNP-PNP). However, the SMF contributes substantially to the warming in the mid-latitude areas where the soil drying is the strongest. Not surprisingly given the non-linear dependence of surface evapotranspiration on soil moisture, the nudging technique has a significant cooling effect in both present-day and future climate simulations. This is due to the lack of strong dry departures from the reference monthly mean soil moisture climatology in the nudged experiments, whereas significant wet departures subsist in case of heavy precipitation (cf. Fig. S1). The SMF contribution to Tmax anomalies is dominated by the changes in latent heat flux (Fig. S2a), the systematic increase of land surface evapotranspiration in FNP versus PNP, being partly or entirely offset by the soil drying in FNF versus FNP. Similarly, precipitation changes are dominated by the SMF in the region of strong drying (Fig. S2b).

Fig. 2 shows the empirical probability density function (pdf) of daily Tmax over central US [105-85°W/32-47°N] and eastern Europe [20-45°E/45-60°N] for all the experiments, as well as for two observational datasets. These two areas of focus were chosen following the same criteria: a strong amplification of global warming and a weak maritime influence, given the lack of SST interaction in our experiments. They show significant biases in the reference (PR) daily Tmax distributions. As confirmed by Fig. S3, such biases are common to many global climate models [e.g., Cattiaux *et al.* 2013, Cheruy *et al.* 2014]. Moreover, they do not show a clear relationship with SMF in the CNRM model (cf. Fig. S4). For these reasons, we do not consider that they represent a major limitation of our study. Overall, climate change

induces a substantial shift and distortion of the temperature pdf in the reference simulations (FR versus PR). In line with Fig. 1, nudging towards a monthly mean soil moisture climatology has a limited impact on the pdf. Interestingly, the climate change simulated without the SMF mainly shows a shift of the pdf towards warmer values (FNP versus PNP), while changes in the shape of the pdf are mainly explained by the SMF (FNF versus FNP). In terms of seasonal mean temperature, the SMF is responsible for about one third of the projected warming over both central US and eastern Europe.

Fig. 3 widens the perspective over the whole Northern Hemisphere and confirms that the SMF plays a key role in reshaping the temperature distributions in the mid-latitudes, while other processes are more relevant in the tropics and high-latitudes. This conclusion is based on the Kolmogorov-Smirnov (KS) statistics, which quantifies the distance between the empirical cumulative distribution functions of two samples. The null distribution of this statistic is calculated under the null hypothesis that the samples are drawn from the same distribution. The two-sample KS test is here applied to daily maximum temperature anomalies after shifting the two distributions by their respective seasonal mean warming and, thereby, to demonstrate significant differences in the shape (rather than the location) of the two distributions. The key role of SMF in reshaping the temperature distribution is strengthened by Fig. S5 and S6 showing mid-latitude changes in both variance and skewness. Fig. 3 also draws attention to a significant (but weaker) nudging effect on the shape of the  $T_{\max}$  distribution, which is not surprising given the damping of both intraseasonal and interannual soil moisture variability. Our results are consistent with the finding of Berg et al. (2014) about the importance of analyzing moments beyond the mean and variance to characterize fully the interplay of soil moisture and near-surface temperature.

Finally, Fig. 4 highlights the SMF contribution to changes in the heat wave characteristics over the central US and eastern Europe. We use the exact same procedure as in *Schoetter et al. [2014]*. A grid cell is considered to experience a heat wave when  $T_{\max}$  exceeds the 98<sup>th</sup> percentile (Q98) of the 1979-2008 distribution. Such a criterion is less sensitive to model biases and domain definition than the use of an absolute temperature threshold. The PNP simulation is taken as the reference to compute Q98, even if the nudging towards a monthly mean soil moisture climatology leads to a slight underestimation of the daily  $T_{\max}$  variability in PNP (FNF) compared to the PR (FR) reference climate simulation, cf. Fig. S5). Then, a regional heat wave event is defined when at least 15% of grid cells encompassed in the spatial domain meet the  $T_{\max}$  threshold criterion for at least three consecutive days. This minimum extent was set in order to get a reasonable sample of heat waves in the present-day PNP simulation. Heat waves separated by one or two days are concatenated. The mean heat wave intensity is then defined as the difference between  $T_{\max}$  and Q98 averaged over the heat wave duration and all grid points affected by the heat wave. The severity of a heat wave is defined as the product of duration, mean extent and mean intensity. The average of the severity across several heat waves is calculated as a geometric mean, as it is less sensitive to very high departures than the arithmetic mean. Finally, a bootstrap procedure is performed to derive 90%-level confidence intervals corresponding to the mean severity: we sample 30 years within the 30 years of simulation (allowing for repetitions), we compute the mean severity over this sample, and we iterate 1000 times in order to empirically estimate the confidence interval. The joint pdf of duration and mean spatial extent shown in Fig. 4 exhibits significant and consistent changes between present-day and future climates over both regions. They are partly explained by the soil drying which accounts for about half of the increase in the mean severity, defined as the product of duration, mean extent and mean intensity. The statistical significance of this contribution is demonstrated by the 5-95% confidence intervals

which do not overlap between FNP and FNF. The mean severity of the reference future climate simulation (FR) is slightly, and not significantly, underestimated by FNF due to the use of climatological, and thus less extreme, soil moisture boundary conditions. The number of heat waves also shows a significant increase due to both SMF (FNF versus FNP) and the rest of climate change (FNP versus PNP), but the number of events estimated over 30 years can be sensitive to the internal variability and/or to spurious effects due to the heat wave definition (e.g., only one heat wave per year if all summer days meet the heat-wave criteria). In summary, Fig. 4 demonstrates that a realistic simulation of both present-day and future soil moisture is a prerequisite for a reliable projection of the summer mid-latitude heat waves in a warmer climate. This conclusion also holds for other heat wave statistics than the mean severity, such as the maximum intensity and maximum extent shown in Fig. S7.

#### **4. Summary and prospects**

To conclude, many processes are likely to contribute to model uncertainties in projected near surface temperatures. They need to be prioritized in order to efficiently constrain global and regional climate projections, as well as related impact studies. While cloud feedbacks have been legitimately put at the top of the climate research agenda given their key influence on global climate sensitivity, other processes are likely to amplify the projected land surface warming and/or to alter the shape of the temperature distribution, both with consequences for extreme events. Our study clearly shows that the SMF represents a significant source of change in the location, scale and shape of the daily Tmax distribution at the regional scale. It is responsible for about half of the projected increase in the severity of boreal summer mid-

latitude heat waves in the CNRM climate model. Given the highly model-dependent response of soil moisture in global climate projections (e.g. Orlowky and Seneviratne 2013), the SMF therefore represents a significant source of uncertainty in the projection of extreme temperatures. Such a conclusion advocates a strong participation to the forthcoming Land Surface, Snow and Soil moisture Model Intercomparison Project (LS3MIP) focusing on land surface feedbacks in global climate projections [Seneviratne *et al.* 2014]. In this context, we advise to pay attention to the experimental design and the possible spurious effects of switching off the high-frequency land-atmosphere coupling for inhibiting the SMF in climate projections. The direct effect of carbon dioxide on plants' transpiration and its possible influence on daily temperatures, not considered in the present study, should also be explored.

**Acknowledgements:** The authors are grateful to Aurélien Ribes for helpful discussions and to Robert Schoetter for the development of heat wave diagnostics in R. The monthly model outputs of our set of simulations are freely available for research purpose. Please, contact Sophie Tyteca (sophie.tyteca@meteo.fr) to access the required list of variables as netcdf files that will be then published on the CNRM-GAME ESGF data node.

## References

Berg, A., B. Lintner, K. Findell, S. Malyshev, P. Loikith and P. Gentine (2014), Impacts of soil moisture-atmosphere interactions on surface temperature distribution, *Journal of Climate*, 27, 7976-7993.

Boberg, F., and J. H. Christensen (2012), Overestimation of Mediterranean summer temperature projections due to model deficiencies, *Nat. Clim. Change*, 2, 433-436, doi:10.1038/nclimate1454.

Boé, J., and L. Terray (2008), Uncertainties in summer evapotranspiration changes over Europe and implications for regional climate change. *Geophys. Res. Lett.*, 35, L05702, doi:10.1029/2007GL032417.

Cattiaux, J., H. Douville, Y. Peings (2013), European temperatures in CMIP5: origins of present-day biases and future uncertainties. *Clim. Dyn.*, 41:2889-2907, doi:10.1007/s00382-013-1731-y.

Cattiaux, J., H. Douville, R. Schoetter, S. Parey, P. Yiou (2015), Projected increase in the daily variability of European summer temperatures. *Geophys. Res. Lett.*, 42, 899-907, doi:10.1002/2014GL062531.

Cheruy, F., J-L. Dufresne, F. Hourdin, A. Ducharne. (2014), Role of clouds and land-atmosphere coupling in mid-latitude continental summer warm biases and climate change amplification in CMIP5 simulations. *Geophys. Res. Lett.*, 41, 6493-6500, doi:10.1002/2014GL061145.

Clark, R.T., J.M. Murphy, S.J. Brown (2010), Do global warming targets limit heatwave risk? *Geophys. Res. Lett.*, 7, L17703, doi:10.1029/2010GL043898.

Diffenbaugh, N. S., and M. Ashfaq (2010), Intensification of hot extremes in the United States. *Geophys. Res. Lett.*, 37, L15701.

Douville, H., F. Chauvin, H. Broqua (2001), Influence of soil moisture on the Asian and African monsoons. Part I: Mean monsoon and daily precipitation. *J Climate*, 14, 2381-2403.

Douville H. (2003), Assessing the influence of soil moisture on seasonal climate variability with AGCMs. *J Hydrometeorology*, 4, 1044-1066.

Fischer, E. M., J. Rajczak, and C. Schär (2012), Changes in European summer temperature variability revisited. *Geophys. Res. Lett.*, 39, L19702.

Hegerl, G. C., F. W. Zwiers, P. A. Stott, and V. V. Kharin (2004), Detectability of anthropogenic changes in annual temperature and precipitation extremes. *Journal of Climate*, 17, 3683-3700.

Orlowsky B. and S. I. Seneviratne (2013), Elusive drought: uncertainty in observed trends and short- and long-term CMIP5 projections. *Hydrol. Earth Syst. Sci.*, 17, 1765-1781, doi:10.5194/hess-17-1765-2013.

Schär, C., P. L. Vidale, D. Lüthi, C. Frei, C. Häberli, M. A. Liniger, and C. Appenzeller (2004), The role of increasing temperature variability in European summer heatwaves. *Nature*, 427, 332-336.

Schoetter, R., J. Cattiaux, H. Douville (2014), Changes of western European heat wave characteristics projected by the CMIP5 ensemble. *Clim. Dyn.*, doi:10.1007/s00382-014-2434-8.

Seneviratne, S.I., D. Lüthi, M. Litschi, and C. Schär (2006), Land-atmosphere coupling and climate change in Europe. *Nature*, 443, 205-209.

Seneviratne, S. et al. (2010), Investigating soil moisture-climate interactions in a changing

climate: A review. *Earth-Science Reviews*, 99, 3-4, 125-161.

Seneviratne, S., and co-authors (2013), Impact of soil moisture-climate feedbacks on CMIP5 projections: First results from the GLACE-CMIP5 experiment. *Geophys. Res. Lett.*, 40, 1–6, doi:10.1002/grl.50956.

Seneviratne, S. and co-authors (2014), Land processes, forcings, and feedbacks in climate change simulations: The CMIP6 LandMIPs. *GEWEX News*, 24, 4, 6-10.

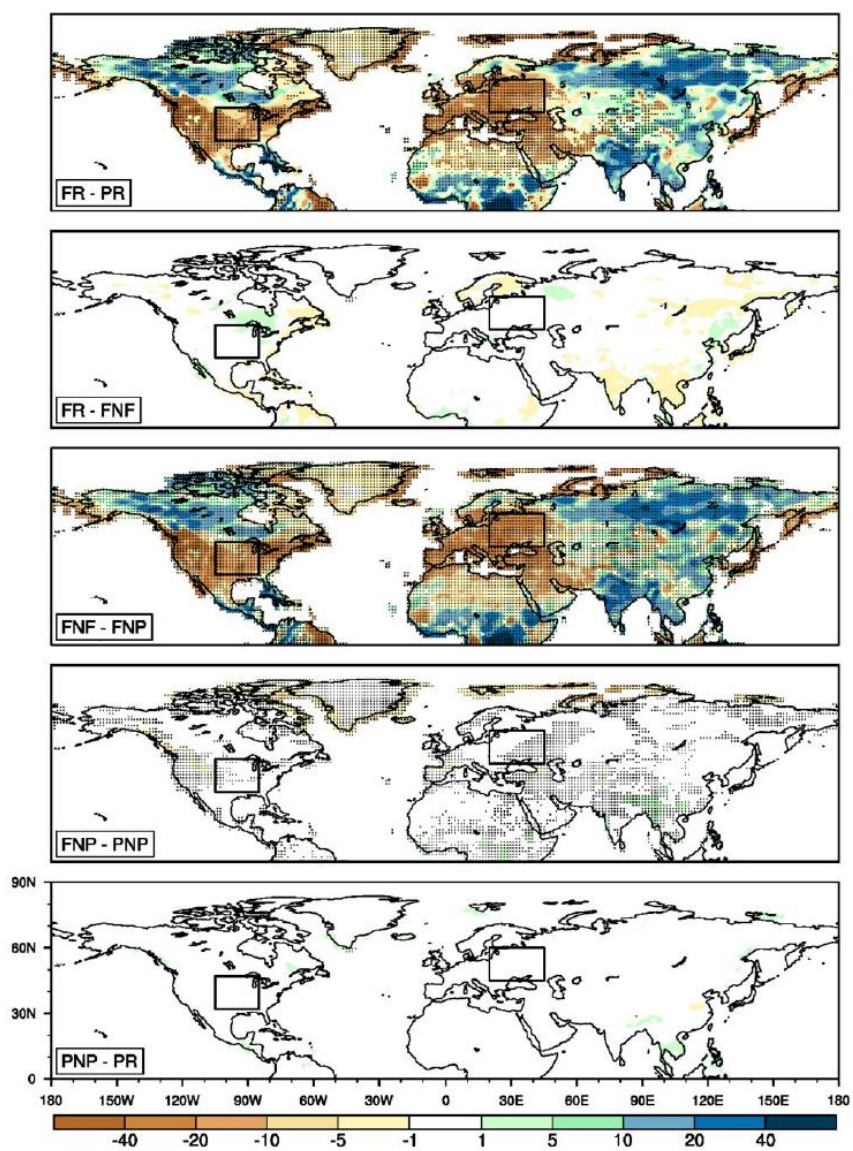
Sillmann, J., V. V. Kharin, F. W. Zwiers, X. Zhang, and D. Bronaugh (2013), Climate extremes indices in the CMIP5 multimodel ensemble: Part 2. Future climate projections. *J. Geophys. Res. Atmos.*, 118, 2473–2493, doi:10.1002/jgrd.50188.

Vial, J., J-L. Dufresne, S. Bony (2013), On the interpretation of inter-model spread in CMIP5 climate sensitivity estimates. *Clim. Dyn.*, 41, 3339–3362, doi :10.1007/s00382-013-1725-9.

Volodre, A. et al. (2013), The CNRM-CM5.1 global climate model: description and basic evaluation. *Clim Dyn.*, doi:10.1007/s00382-011-1259-y.

Volodin, E.M., A.Y. Yurova (2013), Summer temperature standard deviation, skewness and strong positive temperature anomalies in the present day climate and under global warming conditions. *Clim. Dyn.*, 40, 1387-1398.

### Soil Moisture ( $\text{kg.m}^{-2}$ )



## 2-meter daily maximum temperature ( $^{\circ}\text{C}$ )

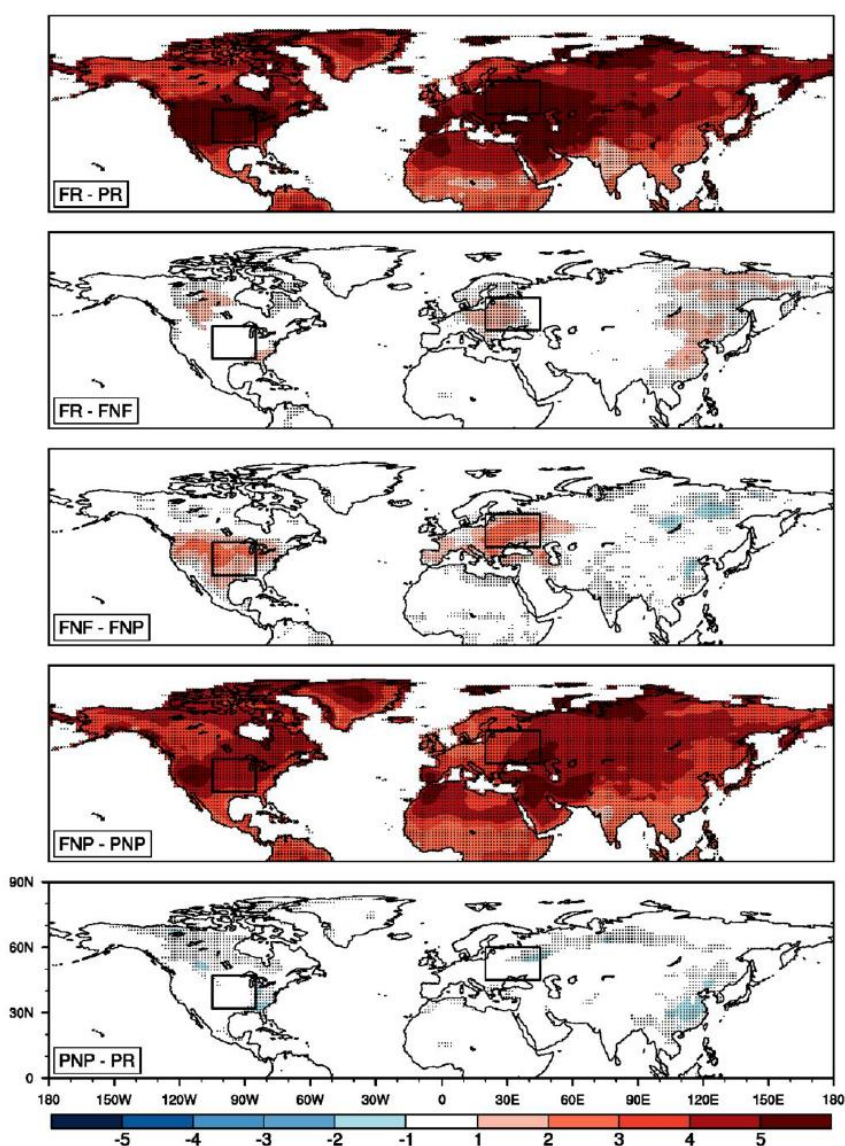
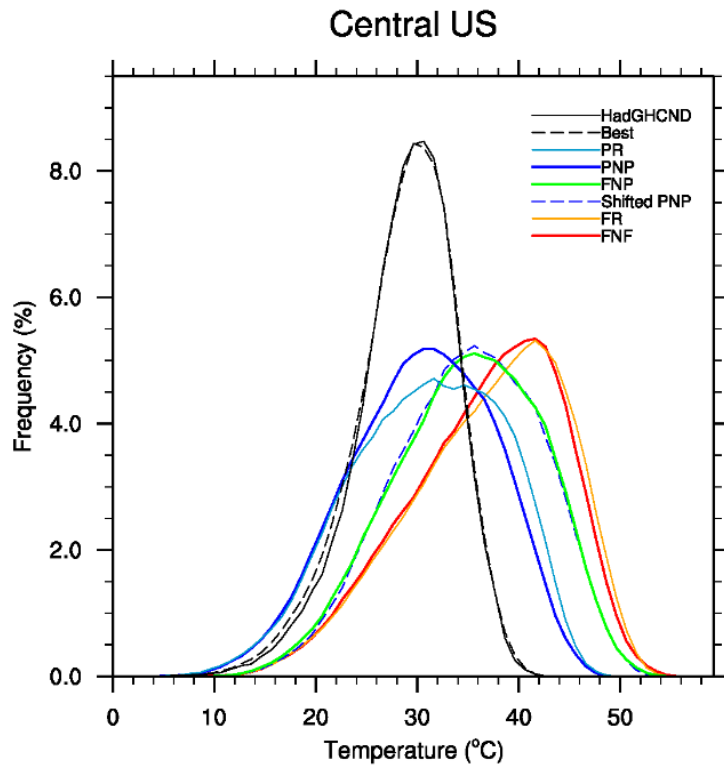
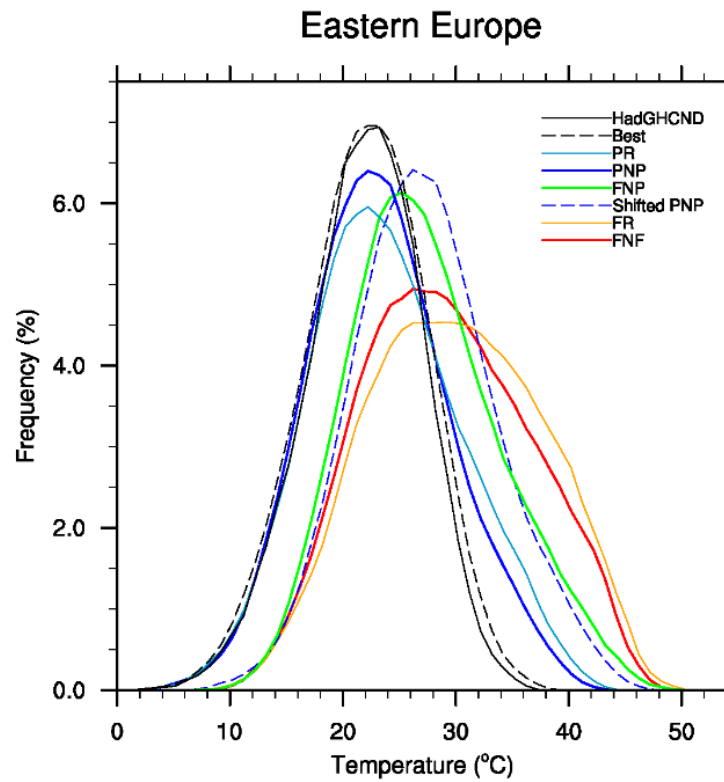


Figure 1: Northern Hemisphere breakdown of summer mean soil moisture (left panels,  $\text{kg}/\text{m}^2$ ) and daily  $T_{\text{max}}$  (right panels, K) anomalies projected in the reference climate change experiments (FR-PR) into 4 contributions: nudging in future climate (FR-FNF), soil moisture feedback (FNF-FNP), climate change without soil moisture feedback (FNP-PNP), and nudging in present-day climate (PNP-PR). Stippling denotes grid cells where anomalies are statistically significant at the 95% level based on a two-sided t-test. Black rectangles denote the central US and eastern Europe domains selected for a regional analysis of the temperature distribution.



(a)



(b)

Figure 2: Empirical distribution of daily Tmax (K) for both present-day and future climate simulations over a) central US [105-85°W/32-47°N] and b) eastern Europe [20-45°E/45-60°N]. Two estimates of the observed pdf, from the Hadley Centre (HadGHCND, <http://hadobs.metoffice.com/hadghcnd/>) and Berkeley (Best, <http://berkeleyearth.org/data/>) gridded datasets respectively, are also shown in black. The dashed blue line is obtained by shifting the PNP distribution by the mean warming between PNP and FNP to demonstrate the lack of change in the distribution shape between present-day and future climates when SMF is not considered.

Accepted Article

### Kolmogorov-Smirnov distance

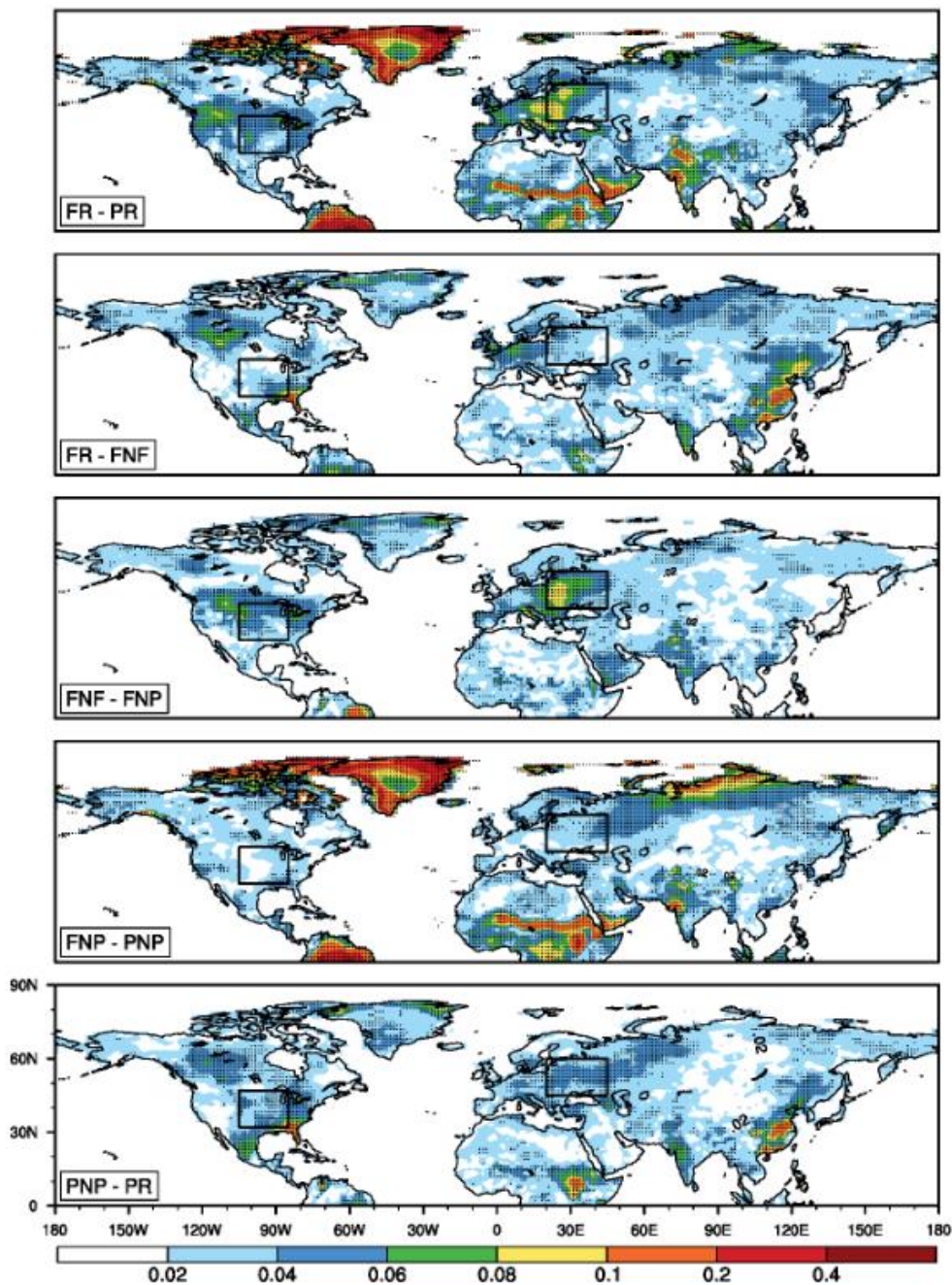
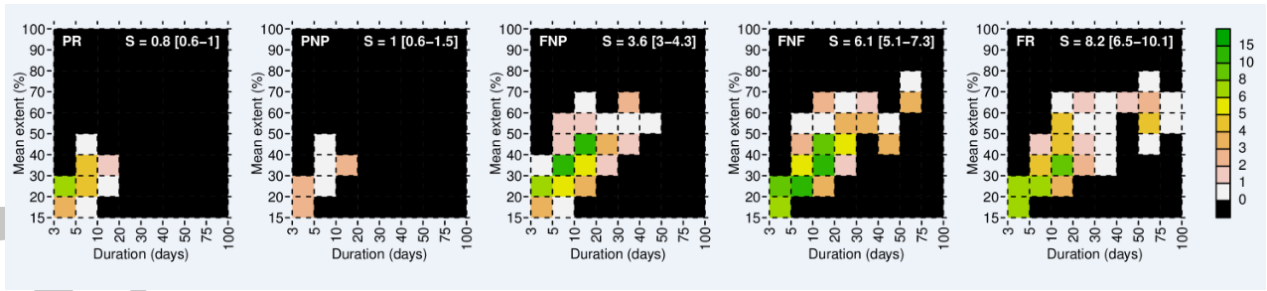
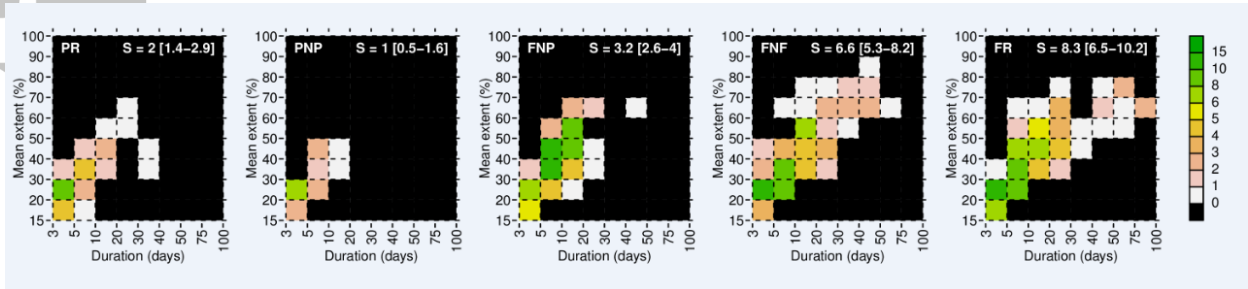


Figure 3: Northern Hemisphere distribution of the Kolmogorov–Smirnov (KS) statistics, which quantifies the distance between pairs of empirical distributions of daily summer Tmax. Stippling denotes grid cells where the distance is statistically significant at the 95% level using a two-sided two-sample KS test. Note that all distributions have been centered (i.e. the summer mean Tmax has been removed) in order to focus on the shape of the distribution.



(a)



(b)

Fig. 4: Joint pdfs of heat wave duration and mean extent for all 30-year simulations (PR, PNP, FNP, FNF and FR from left to right) over a) central US and b) eastern Europe. In each panel,  $S$  denotes the mean heat wave severity with the bootstrapped 5-95% confidence interval in brackets. All severity values have been normalized relative to the mean severity estimated in PNP.